

# Automated Detection of Intracranial Large Vessel Occlusions on Computed Tomography Angiography

## A Single Center Experience

Shalini A. Amukotuwa, MD; Matus Straka, PhD; Heather Smith, RN; Ronil V. Chandra, MD; Seena Dehkharghani, MD; Nancy J. Fischbein, MD; Roland Bammer, PhD

**Background and Purpose**—Endovascular thrombectomy is highly effective in acute ischemic stroke patients with an anterior circulation large vessel occlusion (LVO), decreasing morbidity and mortality. Accurate and prompt identification of LVOs is imperative because these patients have large volumes of tissue that are at risk of infarction without timely reperfusion, and the treatment window is limited to 24 hours. We assessed the accuracy and speed of a commercially available fully automated LVO-detection tool in a cohort of patients presenting to a regional hospital with suspected stroke.

**Methods**—Consecutive patients who underwent multimodal computed tomography with thin-slice computed tomography angiography between January 1, 2017 and December 31, 2018 for suspected acute ischemic stroke within 24 hours of onset were retrospectively identified. The multimodal computed tomographies were assessed by 2 neuroradiologists in consensus for the presence of an intracranial anterior circulation LVO or M2-segment middle cerebral artery occlusion (the reference standard). The patients' computed tomography angiographies were then processed using an automated LVO-detection algorithm (RAPID CTA). Receiver-operating characteristic analysis was used to determine sensitivity, specificity, and negative predictive value of the algorithm for detection of (1) an LVO and (2) either an LVO or M2-segment middle cerebral artery occlusion.

**Results**—CTAs from 477 patients were analyzed (271 men and 206 women; median age, 71; IQR, 60–80). Median processing time was 158 seconds (IQR, 150–167 seconds). Seventy-eight patients had an anterior circulation LVO, and 28 had an isolated M2-segment middle cerebral artery occlusion. The sensitivity, negative predictive value, and specificity were 0.94, 0.98, and 0.76, respectively for detection of an intracranial LVO and 0.92, 0.97, and 0.81, respectively for detection of either an intracranial LVO or M2-segment middle cerebral artery occlusion.

**Conclusions**—The fully automated algorithm had very high sensitivity and negative predictive value for LVO detection with fast processing times, suggesting that it can be used in the emergent setting as a screening tool to alert radiologists and expedite formal diagnosis. (*Stroke*. 2019;50:2790–2798. DOI: 10.1161/STROKEAHA.119.026259.)

**Key Words:** automation ■ computed tomography angiography ■ reperfusion ■ stroke ■ thrombectomy

Large vessel occlusions (LVOs) cause approximately one-third of acute ischemic strokes, yet they are responsible for 90% of mortality related to this condition and severe neurological disability in survivors.<sup>1</sup> Endovascular thrombectomy decreases disability, improves functional outcomes, and decreases mortality over standard medical management in patients with an anterior circulation LVO.<sup>2,3</sup> It is therefore the standard of care treatment for occlusion of the intracranial internal carotid artery (ICA) or the M1 segment of the middle cerebral artery (M1-MCA) and can be performed safely in carefully selected patients up to 24 hours following stroke onset.<sup>4–6</sup>

Given the availability of a highly effective treatment, and the disproportionately high morbidity and mortality when left untreated, detection of LVOs is critically important. An LVO

confirmed on vascular imaging, typically computed tomography angiography (CTA), was a prerequisite for enrollment in the recent thrombectomy trials.<sup>4,5,7–9</sup> The American Heart Association guidelines now recommend vascular imaging in patients who otherwise meet criteria for thrombectomy.<sup>6</sup> CTA is therefore a routine component of the standard of care multimodal stroke computed tomography (CT) protocol that is used to evaluate patients presenting within the thrombectomy window.<sup>6,10</sup>

LVOs are a time-critical emergency for 2 reasons: the thrombectomy window is limited; and LVOs produce large infarcts if timely reperfusion is not instituted to salvage ischemic but viable brain tissue.<sup>11</sup> Prompt diagnosis is therefore imperative, particularly in peripheral centers where rapid identification of an LVO is essential to ensure timely and

Received May 18, 2019; final revision received July 19, 2019; accepted July 25, 2019.

From the Diagnostic Imaging, Monash Health, Clayton, Australia and Department of Radiology, Barwon Health, Geelong, Australia (S.A.A.); Stanford Stroke Center, Stanford University School of Medicine, CA (M.S.); Department of Neurology, Barwon Health, Geelong, Australia (H.S.); Diagnostic Imaging, Monash Health, Clayton, Australia (R.V.C.); Department of Radiology, New York University Langone Medical Center (S.D.); Department of Radiology, Stanford University, CA (N.J.F.); and Department of Radiology, University of Melbourne, Parkville, Australia (R.B.).

**The online-only Data Supplement is available with this article at <https://www.ahajournals.org/doi/suppl/10.1161/strokeaha.119.026259>.**

Correspondence to Shalini A. Amukotuwa, MD, Diagnostic Imaging, Monash Health, Clayton 3168, Australia. Email [samukotuwa@gmail.com](mailto:samukotuwa@gmail.com)

© 2019 American Heart Association, Inc.

*Stroke* is available at <https://www.ahajournals.org/journal/str>

DOI: 10.1161/STROKEAHA.119.026259

appropriate patient referral and transfer to a comprehensive stroke center for treatment.

Clinical decision support tools that automate detection of the infarct core and ischemic penumbra are well established and are used routinely to improve workflow and expedite treatment decisions in acute stroke.<sup>10,12</sup> Automation is now being applied to the task of detecting intracranial LVOs in a clinically acceptable timeframe to further support these goals.

The aim of this study was to evaluate the accuracy and speed of an automated tool (RAPID CTA) for detection of intracranial anterior circulation LVOs in a cohort of consecutive patients presenting to a regional hospital with suspected acute ischemic stroke. The primary outcome was the diagnostic performance for detecting intracranial LVOs, measured against the reference standard of experienced neuroradiological interpretation. We hypothesized that the automated software was able to detect an LVO with a sensitivity of >90%, a negative predictive value (NPV) >95%, and a specificity of at least 70%. This hypothesis was based on the target sensitivity and NPV of the developers (the FDA typically requires a sensitivity of >90% for CADx devices) and early prerelease testing of the software.

## Methods

The data that support the findings of this study are available from the corresponding author on reasonable request.

Consecutive patients who presented to our institution between January 1, 2017 and December 31, 2018 underwent multimodal brain CT for a suspected acute ischemic stroke and met the following inclusion criteria were retrospectively identified using our Picture Archiving and Communication System and electronic medical records. The inclusion criteria were (1) patient  $\geq 18$  years old and (2) multimodal stroke protocol CT performed within 24 hours of symptom onset or last seen well. Exclusion criteria were (1) technically inadequate CTA (poor contrast bolus or substantial motion or metal artifact that precluded accurate assessment of the intracranial arteries to the level of the distal M2 segments of the middle cerebral arteries by an experienced neuroradiologist) and (2) thin slice CTA images unavailable. The justification for these exclusion criteria were (1) the CTA had to be of sufficient quality for accurate interpretation by an experienced human reader, the reference standard against which the LVO-detection algorithm was assessed, and (2) thin slice high-resolution images were necessary for processing by the algorithm.

The study was approved by the local institutional review board, which granted a waiver of written consent based on the retrospective study design and anonymization of all data. This investigator-initiated study received no financial support.

## CT Image Acquisition and Reconstruction Technique

All patients were scanned on a 256-slice multi-detector CT (iCT 256, Philips Healthcare, Cleveland, OH). Our institution's routine multimodal stroke CT protocol consisted of unenhanced CT followed by CT perfusion (CTP) and CT angiography (CTA).

Unenhanced CT was acquired in the helical mode with the following parameters: 0.625 mm slice collimation, spiral pitch factor of 0.283, tube voltage of 120 kV, and image matrix 512 $\times$ 512. Images were reconstructed using a UB kernel at 1 mm overlapping sections, with axial, coronal, and sagittal multiplanar reconstructions performed at 4 mm slice thickness.

Fifty milliliters of nonionic contrast agent (350 mg iodine/mL iohexol [Omnipaque 350], GE Healthcare, WI) was injected intravenously for CTP (see the [online-only Data Supplement](#) for technique).

For the subsequent CTA, 80 mL of the same nonionic contrast agent was injected intravenously at a rate of 5 mL/s followed by a 40 mL saline flush at 6 mL/s. Contrast bolus triggering was performed

in the aortic arch. Parameters for the helical acquisition were as follows: craniocaudal coverage from the aortic arch to vertex, 100 kV tube voltage with dose modulation, slice collimation width 0.625 mm, image matrix 512 $\times$ 512, and spiral pitch factor 0.618. The following reconstruction parameters were used: iterative reconstruction (iDose) factor of 5 and convolution kernel B. Axial images were reconstructed at 0.8 mm overlapping sections. Axial, coronal, and sagittal multiplanar reconstructions were performed at 4 mm slice thickness. Axial maximum intensity projections were reconstructed at 10-mm thickness.

## LVO Definitions

For this study, the term intracranial LVO was used specifically to describe anterior circulation occlusions involving the M1-MCA and the intracranial ICA (from the petrous segment to the ICA bifurcation<sup>13</sup>). Supracaloid ICA refers to the ophthalmic and communicating segments.

The M1-MCA was defined functionally as the segment from the ICA bifurcation to the MCA bifurcation or trifurcation. The M2 segments were defined as those immediately distal to the MCA bifurcation/trifurcation that ascend vertically within the Sylvian fissure (assessed on coronal images).<sup>14</sup> Proximal M2 occlusions were defined as being located inferior to a transverse plane drawn through the mid-point of the Sylvian cistern on coronal images. The dominance of an M2 segment was assessed based on its size relative to the other M2 segment(s) and the extent of the perfusion abnormality it produced.<sup>14</sup>

When there was early division of the MCA, a functional rather than traditional angiographic definition was adopted; the short proximal trunk was called the M1 segment and the branches distal to division were defined as M2 segments.

## Image Analysis

Two diagnostic neuroradiologists (Dr Amukotuwa and SD, with 8 and 9 years of post-fellowship experience, respectively) reviewed each patient's complete multimodal CT: the unenhanced CT, CTP, and CTA. Details of the patient's clinical presentation were provided. The technical adequacy of the CTA was first assessed. The following features were then recorded in consensus (and subsequently verified by an interventional neuroradiologist [RVC] with 7 years' experience):

The presence, side, and site of an intracranial LVO.

The presence, side, and site (proximal versus distal) and dominance of a M2-MCA occlusion.

For tandem lesions, each site of occlusion was recorded. For M1-MCA occlusions, the length of the nonopacified vessel segment was recorded.

These neuroradiologist reads served as the reference standard against which the performance of the automated LVO detection tool was assessed.

## LVO Detection Using Automated Software

An automated tool (RAPID CTA, RAPID 4.9, iSchemaView, Menlo Park, CA) was used to analyze each patient's CTA raw data for the presence and side of an LVO.

The RAPID CTA algorithm performs the following operations: (1) imports the CTA raw data in Digital Imaging and Communications in Medicine format; (2) motion and tilt corrects the images; (3) trims the CTA data craniocaudally to restrict coverage from the C1 vertebra to the vertex; (4) elastically aligns an anatomic template of the human head with the CTA data; (5) warps templates of relevant anatomic structures (eg bones and blood vessels) onto the CTA to create masks; (6) removes the skull base and calvarium using the bone mask; (7) identifies intracranial vessels and dichotomizes them into small and large diameter groups; (8) determines the vessel density by assessing the length of large caliber vessels in the suprasellar cistern (supracaloid ICA) and proximal Sylvian cistern (M1-MCA) as well as the sum of density values (in Hounsfield units) of the voxels constituting these vessels; (9) determines vessel density for small caliber vessels (distal M1, M2, and M3 segments) further distally in and adjacent to the Sylvian

cisterns; (10) performs left-right comparison to determine the relative vessel density ratio, first within the suprasellar and proximal Sylvian cistern, then progressing further distally; (11) creates axial, coronal, and sagittal maximum-intensity projections of the intracranial vasculature from the bone-masked CTA; (12) highlights the areas of reduced relative interhemispheric vessel density on these MIPs applying the following color-coded thresholds: 75% to 80% (blue), 60% to 74% (green), 45% to 59% (yellow), and <45% (red; Figure 1); and (13) sends these MIPs as de-identified output maps to the picture archiving and communication system. Application of the 4 different thresholds is simultaneous and fully automated.

The processing time taken to complete these steps was recorded for each patient. No further training of the algorithm occurred during the study period.

## Statistical Analysis

All statistical analyses were performed using a software package (MedCalc Version 17.2, MedCalc Software bvba, Ostend, Belgium, 2017).

Receiver operating characteristic (ROC) analysis was performed to determine the sensitivity, specificity, positive predictive value, NPV and area-under-the ROC curve of the algorithm for detection of:

An intracranial LVO; and

Either an intracranial LVO or M2 segment occlusion.

A vessel density threshold of <75% (inclusive of the 60%–75%, 45%–59%, and <45% thresholds) was used in this study for LVO detection, as this was recommended by the software developers based on their prerelease testing.

CI's were calculated using a bootstrap procedure with 10000 samples with replacement.

## Results

Five hundred one consecutive patients meeting the inclusion criteria had undergone a multimodal CT with CTA and CTP between 1/1/2017 and 31/12/2018. Eight were excluded because of a technically inadequate CTA (poor contrast bolus in 5 and severe motion degradation in 3). Sixteen (including 2

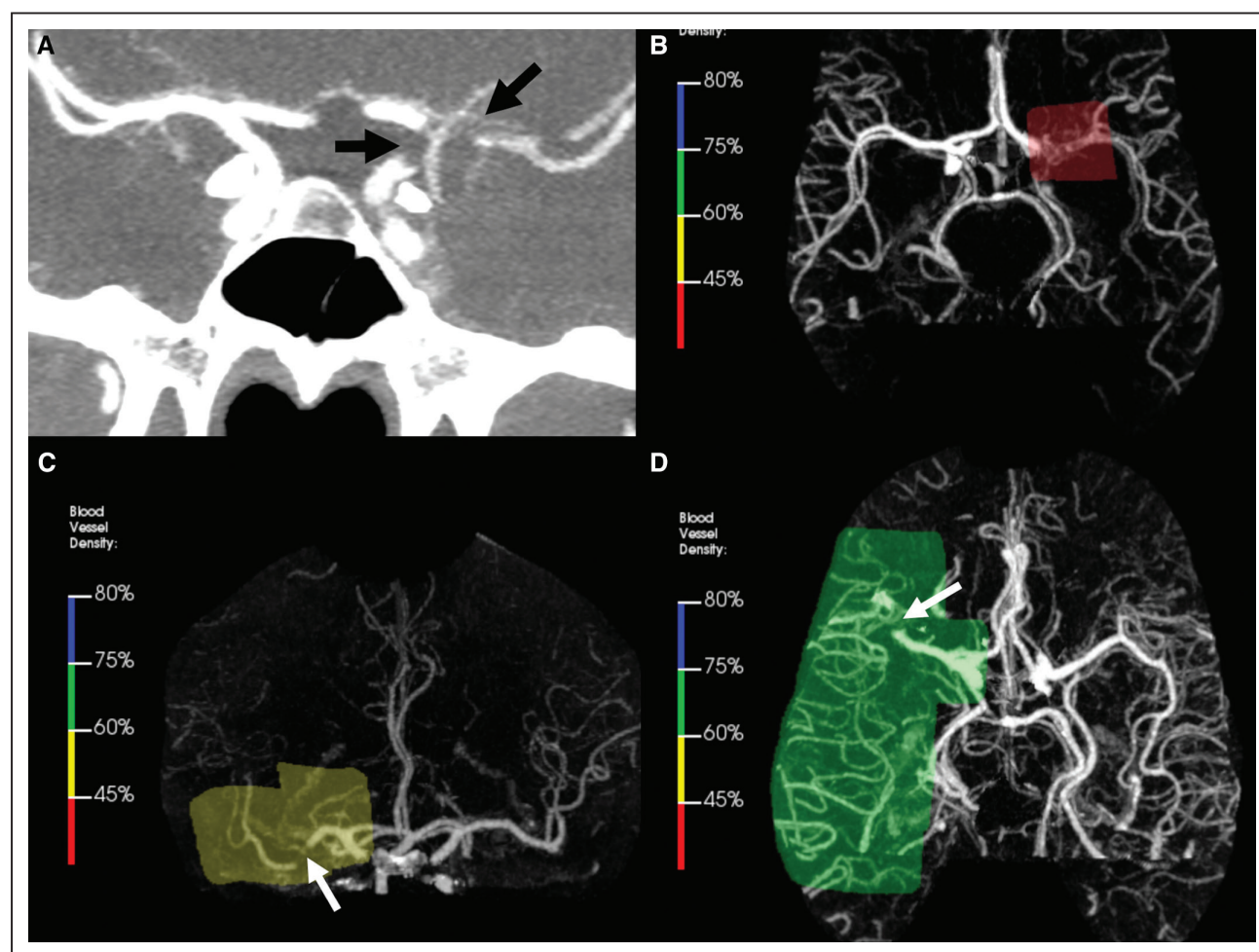


**Figure 1.** Examples of large vessel occlusion detection by the algorithm (an expanded version is shown in Figure III in the [online-only Data Supplement](#)).

**A**, Coronal computed tomography angiography maximum intensity projection (MIP) shows terminal internal carotid artery and proximal M1 segment of the middle cerebral artery (M1-MCA) occlusion (arrows) in a 44 y-old woman who presented with sudden onset right-sided weakness and dysphasia. **B**, The resulting severe vessel density reduction (to <45% contralateral) in the suprasellar cistern allowed the algorithm to detect an large vessel occlusion. Software output of an axial bone-masked MIP with the area of vessel density reduction highlighted in red. **C**, Eighty-eight-year-old woman who presented with sudden onset left-sided weakness. Software output of a coronal MIP showing short-segment distal right MCA-M1 occlusion (arrow) with the area of vessel density reduction highlighted in yellow (<60% contralateral). One of the M2 segments was opacified distal to the occlusion, therefore the vessel density reduction was less than in the previous case necessitating use of a higher threshold. **D**, Sixty-one-year-old man presenting with sudden onset left-sided weakness. Software output showing a short-segment distal right M1-MCA occlusion (arrow) with the area of vessel density reduction highlighted in green (<75% contralateral). Sampling of a larger region was required to identify vessel density reduction, which was less marked than in the previous examples due to good opacification of the M2 and M3 segments distal to the short segment occlusion (indicating good collaterals). The pseudocontrast because of color overlays make the vessels seem more conspicuous than on corresponding conventional MIPs.



with an LVO) were excluded because thin-slice CTA was unavailable on PACS (Patient selection flowchart shown in Figure I in the [online-only Data Supplement](#)).

CTAs from 477 patients were analyzed: 271 male (median age, 70; IQR, 59.5–79) and 206 female (median age, 71.5; IQR, 60–83). Patients' baseline characteristics and the details of vessel occlusion are shown in Tables 1 and 2, respectively.

All cases were processed in under 5 minutes. The mean processing time was 158 seconds (IQR, 150–167 seconds).

### Intracranial LVO Detection

The results of ROC analysis for LVO detection are given in Table 3.

Of the 78 patients with an LVO in the study population, 73 (93.6%) were correctly identified by the algorithm, yielding a sensitivity of 0.94 (95% CI, 0.86–0.98), specificity of 0.76 (95% CI, 0.72–0.80), and NPV of 0.98 (95% CI, 0.96–0.99). The ROC curve is shown in Figure IIA in the [online-only Data Supplement](#).

On post hoc analysis, the algorithm did not miss any LVO associated with poor collateral status (indicated by lack of opacification of the M2 and M3 segments distal to the LVO).

### ICA Occlusions

An LVO was correctly identified in 31/32 (96.9%) patients with an intracranial ICA occlusion. There were 11 patients with a tandem ICA and M1-MCA occlusion and 14 patients with an isolated supraclinoid ICA occlusion that involved the ICA terminus. These were all correctly identified using the <45% threshold (example shown in Figure 1A and 1B).

In 3 patients with proximal supraclinoid ICA occlusions, the ICA terminus and M1-MCA were opacified by cross-flow via the patent anterior communicating segment. In these patients, the proximal part of the supraclinoid ICA was not opacified, resulting in reduction in the vessel density ratio that allowed detection by the algorithm, albeit using a higher threshold of <60%.

The algorithm correctly identified 3 out of 4 petrous-cavernous segment ICA occlusions using the <45% threshold. In these patients, the caliber and luminal density of the supraclinoid ICA was sufficiently reduced compared with the contralateral side (Figure 2) to allow detection. In the remaining patient with a petrous segment ICA occlusion, which was missed by the algorithm, the supraclinoid ICA was well opacified, with no reduction in caliber or luminal density because of collateral supply from the external carotid artery via the ophthalmic artery.

### M1 Occlusions

Of the 46 patients with an isolated M1-MCA occlusion, 42 (91.3%) were correctly identified by the algorithm. Thirty-three were identified using the <45% (red) threshold, whereas 5 were identified using the <60% (yellow) threshold and 4 were identified using the <75% (green) threshold.

Of the 9 patients who were identified using the green or yellow thresholds, 6 had short segment occlusions (measuring <8 mm in length). These patients had good opacification of the M2 segments distal to the occlusion (therefore a smaller relative vessel density reduction), indicating good collateral status. Two examples are shown in Figure 1C and 1D. The remaining 3 patients also had good collaterals as indicated by reconstitution of the proximal M2 segments.

Four M1-MCA occlusions were missed: one incomplete, one short segment (5 mm length), and the other 15 mm long with reconstitution of the proximal M2 segments via collaterals. The remaining case was a long-segment proximal M1-MCA occlusion with reconstitution of the anterior temporal branch and proximal M2 segments, again indicating good collateral status.

### LVO and M2-MCA Occlusion

The results of ROC analysis for detection of either an LVOs or an M2-MCA occlusion are given in Table 3 (the ROC curve is shown in Figure IIB in the [online-only Data Supplement](#)). The sensitivity of 0.92 (95% CI, 0.86–0.96) was lower than for purely LVO detection but the specificity of 0.81 (95% CI, 0.77–0.85) was higher. The NPV was 0.97 (95% CI, 0.95–0.98).

Of the 28 M2-MCA occlusions, 4 were not detected: 2 short-segment proximal occlusions with good collaterals (indicated by opacification of the M2 segment further distally), a small nondominant M2 segment occlusion and a distal nondominant M2 occlusion.

### False Positives

There were 71 false positives. A cause of asymmetrical vascular density in the supraclinoid and Sylvian cisterns was identified in 64 of these patients. Ipsilateral decreased vascular density was caused by: chronic M1-MCA stenosis (n=5); high-grade supraclinoid ICA stenosis (n=1); cervical ICA occlusion with decreased density and caliber of the supraclinoid ICA (n=1); old ipsilateral MCA territory infarction with attenuation of the M1 or M2 segments (n=4); and early bifurcation of the MCA (n=12). False positives also resulted from the following causes

Table 1. Patient Characteristics

	Number	Age, y	NIHSS Median (Interquartile Range)	Male	Intravenous-TPA Given	Thrombectomy Performed
All patients	477	71 (60–80)	6 (2–9)	271 (56.8%)	68	57
Intracranial anterior circulation large vessel occlusion	78	74 (65–82)	14 (10–18)	46 (59.0%)	39	52
M2 segment middle cerebral artery occlusion	28	78 (70–88)	7 (5–11)	12 (42.9%)	2	2
No intracranial anterior circulation large vessel or M2 occlusion (controls)	371	70 (58–80)	4 (1–7)	213 (57.4%)	27	0

NIHSS indicates National Institutes of Health Stroke Scale; and TPA, tissue-type plasminogen activator.

**Table 2. Site of Anterior Segment LVO and M2 Segment Middle Cerebral Artery Occlusion**

		Number
LVO		78
	M1 segment middle cerebral artery only	46
	Intracranial internal carotid artery only	21
	Supraclinoid, including terminus	14
	Supraclinoid, proximal to terminus	3
	Petrous-Clinoid segments	4
	Tandem M1-middle cerebral artery and intracranial internal carotid artery	11
M2 segment of middle cerebral artery occlusions		28
Location	Proximal	24
	Distal	4
Division	Both	4
	Dominant	13
	Co-dominant	4
	Nondominant	7

LVO indicates large vessel occlusion.

of contralateral increased vascular density (Figure 3): a large anterior temporal branch (n=7); asymmetrically large or unilateral posterior communicating segment (n=15); hyperperfusion (n=3: 2 patients with hypervascular tumors and 1 with seizures); large MCA aneurysm (n=1); large supraclinoid ICA supplying both anterior cerebral arteries (n=2); and opacified venous structures (n=13).

### Cervical ICA Occlusions

There were 8 patients who had an isolated cervical ICA occlusion. The algorithm diagnosed an intracranial LVO in one of these patients whose supraclinoid ICA was decreased in density (15%) and caliber (50%) compared with its contralateral counterpart. The ipsilateral supraclinoid ICA had only mildly decreased density and caliber in the remaining 7 patients.

### Discussion

This study retrospectively evaluated the performance of an automated LVO detection tool in a cohort of consecutive patients who underwent multimodal CT for a suspected acute ischemic stroke at a regional hospital. Our results demonstrate that a fully automated software algorithm can detect intracranial anterior circulation LVOs with high diagnostic sensitivity (0.94) and NPV (0.98), and moderately high specificity (0.76), confirming our hypothesis. The study also shows that the computing times are short, making this tool suitable for emergent radiological screening.

The sensitivity of the algorithm falls within the range previously reported for neuroradiologists of varying levels of experience (0.94–1.0).<sup>15,16</sup> The specificity is, however, much lower than 0.95 to 0.98 achieved by experienced human readers.<sup>15,16</sup> Vascular asymmetry, which caused most false

positives, can be easily distinguished from an LVO by radiologists and neurologists. We therefore do not advocate replacing experienced human readers with the automated LVO detection tool. Instead, given its high NPV, we propose using this software as a clinical decision support tool to screen the multimodal CTs of stroke patients.

It can alert the treating neurologist and reporting radiologist of a potential LVO and expedite diagnosis by prompting evaluation of the patient's imaging as a high priority. Such a tool would be particularly valuable in regional and peripheral centers such as ours, which do not have the resources and experienced staff to provide around-the-clock on-site multimodal stroke CT interpretation. While all CTAs are ultimately read by a radiologist, they are not always assigned the highest priority, especially after-hours where resources are limited. Often, there is only one on-call radiologist or resident at smaller centers and in countries where subspecialist radiology is not practiced. In this setting, other emergent scans such as trauma may be prioritized ahead of a stroke patient's multimodal CT, resulting in delayed diagnosis. The authors have encountered this issue repeatedly in clinical practice. The algorithm fully automates LVO detection and generates an output within 3 minutes in 75% of cases (and 5 minutes in all cases). This ensures that the positive findings are brought to the reporting radiologist, teleradiologist, or resident's attention within 5 minutes of scanning, which in turn expedites diagnosis. Currently, assessment is often delayed until CTA reformats are completed and the study posted to the radiologist worklist by the CT technologist.

An added benefit of the algorithm for hospitals such as ours that do not have an on-site thrombectomy service is notification of the nearest thrombectomy center. This in turn expedites mobilization of the clot retrieval team and treatment of eligible patients, thereby ensuring the best possible outcomes. Notification is currently reliant upon the local neurologist or emergency physician contacting the thrombectomy center, which can add to delay.

The algorithm may also be a valuable diagnostic support tool. While experienced neuroradiologists have a high sensitivity for detection of LVOs, reported to be 75% to 98%, the diagnostic performance of neurologists and trainees may be considerably lower (63% in 1 study).<sup>15–17</sup> At many centers around the world, such as ours, the acute review of multimodal stroke CTAs is performed by trainee radiologists and neurologists, and these studies are second read by a radiologist (often a generalist) at a later time. Also, even experienced radiologists do miss LVOs.<sup>15</sup> The tool can prompt a second look in these cases, potentially averting a clinically significant miss and consequent harm. While the cost of the software is low, that of a missed or delayed diagnosis of an LVO, where the patient misses out on beneficial treatment and suffers significant neurological disability, is high. Therefore, while we have not performed a specific intervention to assess whether or not the use of the LVO detection software is cost effective, our experience with delayed and missed diagnosis of LVOs suggests that it is.

To our knowledge, there is no previously published complete study that has evaluated the diagnostic performance of an automated LVO-detection algorithm. Two abstracts are available for evaluation of another LVO-detection software<sup>18,19</sup>: the

**Table 3. Results of Receiver Operating Characteristic Analysis for LVO Detection at the Optimal Threshold (<75%)**

Site of Occlusion	Sensitivity*	Specificity*	PPV*	NPV*	Youden*	AUC*
Intracranial large vessel (n=78)	0.94 (0.86–0.98)	0.76 (0.72–0.80)	0.43 (0.39–0.48)	0.98 (0.96–0.99)	0.70 (0.62–0.76)	0.85 (0.81–0.88)
M2-segment middle cerebral artery (n=28)	0.86 (0.67–0.96)	0.68† (0.63–0.72)	0.14† (0.12–0.17)	0.99† (0.97–1.00)	0.54 (0.36–0.64)	0.77 (0.70–0.84)
Intracranial large vessel or M2 segment middle cerebral artery (n=106)	0.92 (0.85–0.96)	0.81 (0.77–0.85)	0.58 (0.52–0.63)	0.97 (0.95–0.98)	0.72 (0.65–0.79)	0.86 (0.83–0.90)

AUC indicates area-under-the ROC curve; NPV, negative predictive value; LVO, large vessel occlusion; and PPV, positive predictive value.

\*Values within parentheses represent the 95% CI.

†With LVOs included. Sensitivity, specificity, PPV, and NPV were 0.86, 0.81, 0.25, and 0.99, respectively when the 78 patients with LVOs were excluded from analysis.

sensitivity of 0.85 to 0.97 reported in these abstracts is comparable to ours, while the reported specificity had a wide range (0.52–0.83). The cohort of patients in those investigations was randomly selected from acute ischemic stroke patients at a number of comprehensive stroke centers and enriched with LVOs. Our study cohort consisted of consecutive patients presenting to a regional hospital with a suspected acute ischemic stroke and is therefore likely to be more heterogenous, with a lower prevalence of LVOs because clinical triage is less refined than at a comprehensive stroke center. By using a non-curated dataset, we have tested our algorithm and determined its diagnostic performance in a real-world context. Our study cohort is also felt to be more representative of the target population for LVO-detection tools.

The LVO detection algorithm evaluated in this study detects hemispheric differences in vessel density within the suprasellar and Sylvian cisterns. Vessel density is affected by the length, caliber, and number (spatial density) of opacified vessels as well as the density of luminal opacification (measured in

Hounsfield units). An LVO results in vessel nonopacification, which in turn reduces ipsilateral vessel density. The resultant asymmetry is detected by the algorithm. For example, supraclinoid ICA occlusions involving the ICA terminus were all detected by the algorithm, using the <45% threshold. In these patients, nonopacification of the supraclinoid ICA and at least the proximal part of the M1-MCA resulted in severe vessel density reduction. Similarly, patients with tandem M1-MCA and intracranial ICA occlusions, who had extensive arterial nonopacification, were detected using the <45% threshold. Patients with an ICA occlusion that spared the terminus, who also had a patent anterior communicating segment, displayed milder vessel density reduction because cross-flow opacified the distal supraclinoid ICA. The vessel density reduction was sufficient for the algorithm to detect an LVO but required use of a higher threshold in these patients.

False negatives for LVO detection could be explained by insufficient relative vessel density reduction to allow detection by the algorithm. This occurred with short-segment

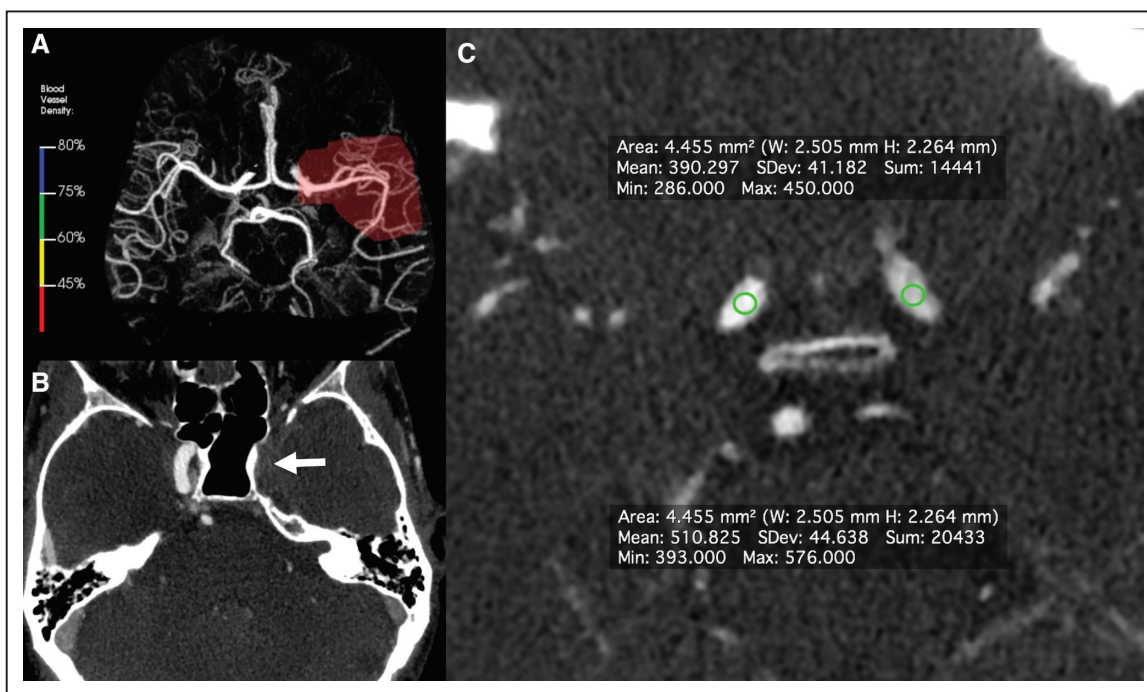


**Figure 2.** Fifty-nine-year-old man with a left petrous internal carotid artery (ICA) occlusion secondary to dissection. **A**, Software output with an axial bone-subtracted maximum intensity projection (MIP). Vessels in the suprasellar and Sylvian cisterns are highlighted in red, indicating severe density reduction compared with the contralateral side despite the normal appearance on the MIP. **B**, Axial 0.8 mm computed tomography angiography showing nonopacification of the left cavernous ICA (arrow). **C**, The left supraclinoid ICA had a lower luminal density (mean density 390 Hounsfield units, top text box) than the right (mean density 510 Hounsfield units, bottom text box), which allowed the algorithm to detect the large vessel occlusion (LVO).



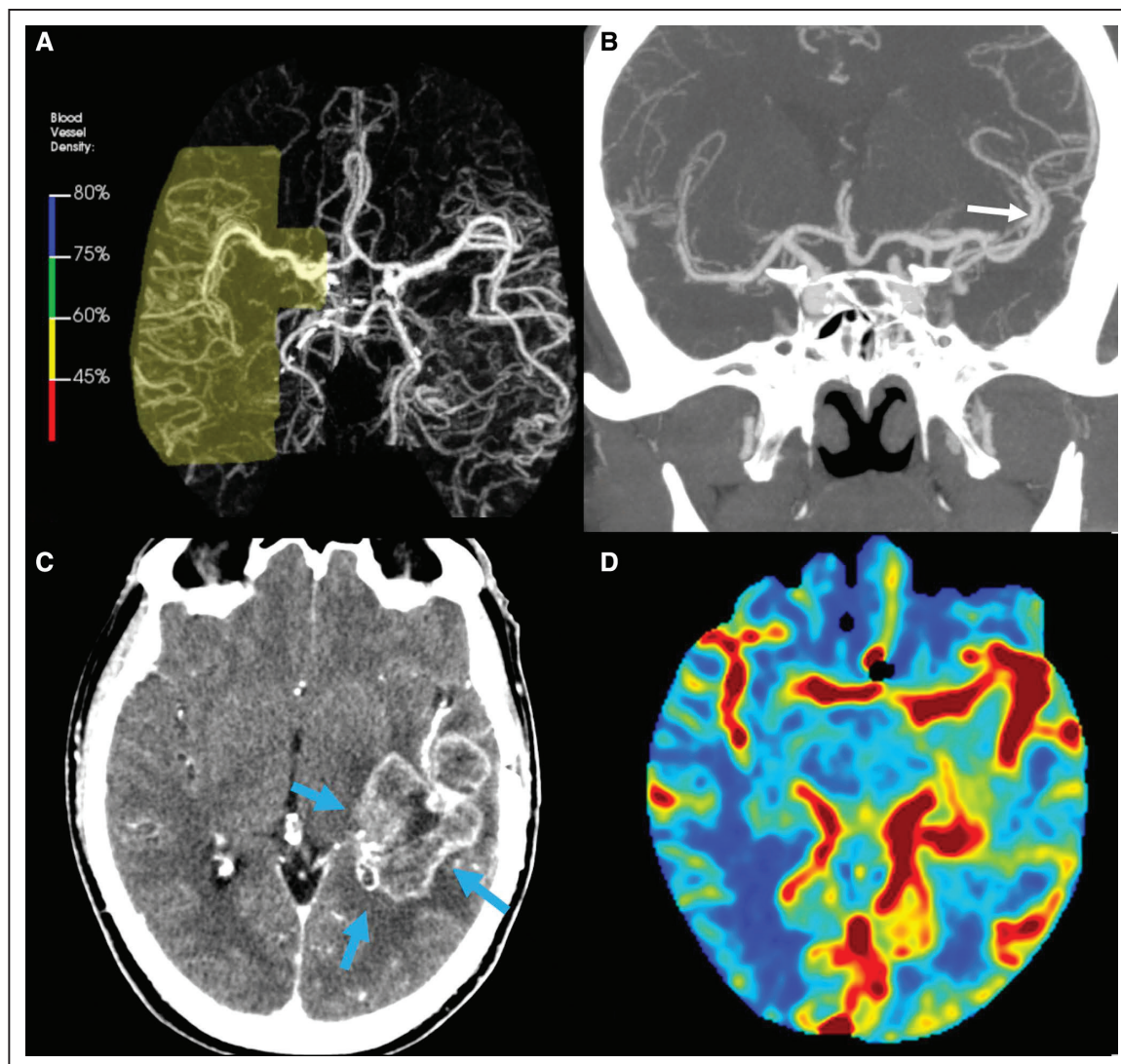


**Figure 3.** Example of a false positive in a 50-y-old man presenting with dysphasia and right-sided weakness. **A**, Software output showing right-sided vessel density reduction to <60% contralateral when vessels in the suprasellar and Sylvian cistern are interrogated. **B**, Coronal computed tomography angiography maximum intensity projection (MIP) (20 mm) showing an increase in vessels in the left Sylvian cistern. **C**, Contrast-enhanced computed tomography axial image showing the causative hypervascular tumor (glioblastoma, arrowed) in the left temporal lobe and insula. **D**, Elevated relative cerebral blood flow and engorgement of the ipsilateral middle cerebral artery are seen on the blood flow map.

(Figure IV in the [online-only Data Supplement](#)) and incomplete M1-MCA occlusions, and in patients with good collaterals where there was M1 or M2 segment opacification distal to the occlusion. High collateral grade, with vessel opacification distal to the occlusion (therefore a smaller reduction in relative vessel density), also accounted for the nine M1-MCA occlusions that were not detected using the lowest (<45%) threshold. These patients with robust collaterals are more likely to be slow progressors whose infarct growth is less time sensitive.<sup>20</sup> Expediting detection may therefore be less critical in this group. None of the patients in whom the algorithm missed an LVO had a poor collateral grade. Poor collaterals are associated with fast progression; therefore, this is the group in which fast diagnosis is most important since rapid reperfusion is necessary for tissue salvage.<sup>20,21</sup>

The only other false negative was a petrous ICA occlusion, which highlights an important limitation of the algorithm. Petrous-clinoid ICA occlusions cannot be directly

detected because of poor performance of the bone mask at the skull base. The supraclinoid ICA was normally opacified in this patient, precluding detection by the algorithm. While the number of patients (4) with skull-base ICA occlusions in this study was too small for meaningful analysis of the accuracy of the LVO-detection tool in this group, it is also reflective of the low prevalence of petrous-clinoid ICA occlusions in the acute ischemic stroke population. Cervical ICA occlusions also pose a challenge for the algorithm because the neck vessels are not interrogated, and these occlusions do not necessarily result in reduced density or caliber of the supraclinoid ICA. Current guidelines do not indicate thrombectomy for patients with isolated cervical ICA occlusions, therefore identifying these using the LVO-detection tool is perhaps less critical at present. It is important that radiologists and neurologists are cognizant of the presence and causes of false negatives and remain vigilant in their interpretation of CTAs even when the algorithm gives a negative result.

The algorithm was able to detect most M2-MCA occlusions. While sensitivity decreased slightly to 0.92, specificity increased to 0.81 and NPV remained approximately stable when M2-MCA occlusions were included. There is evidence of improved functional outcomes with thrombectomy compared with standard medical management in patients with M2-MCA occlusions.<sup>22</sup> Current guidelines therefore state that endovascular thrombectomy can be considered in carefully selected patients with M2-MCA occlusions.<sup>6</sup> In particular, thrombectomy may be justified to achieve rapid reperfusion in patients with severe neurological deficits and ischemia of highly eloquent brain regions. In addition, in patients with M2-MCA occlusions who are ineligible for intravenous thrombolysis (eg, because of presentation beyond the 4.5 hours window), thrombectomy is the only available reperfusion therapy. It could therefore be argued that an LVO-detection tool should also identify M2-MCA occlusions.

False positives were caused by vascular asymmetry related to developmental variants (eg, early unilateral bifurcation of the ipsilateral MCA, which produces asymmetry in vessel caliber, and a unilateral or large contralateral posterior communicating segment), chronic steno-occlusive disease, and contralateral hyperperfusion (eg, because of hypervascular tumors). Since the algorithm does not differentiate between venous and arterial structures, asymmetry in venous structures such as the deep and superficial middle cerebral veins can cause false positives. This can be avoided by measures that prevent venous contamination of the CTA such as rapid contrast bolus injection and performing CTA before CTP.

A limitation of this study is that it is a single-center experience. Further investigation of the utility of the tool in a multicenter study that involves multiple regional spoke hospitals and a clot retrieval hub is planned.

## Conclusions

The algorithm evaluated in this study had high sensitivity and NPV for LVO detection in a cohort of patients who underwent multimodal CT for a clinically suspected stroke. M2-MCA occlusions were also reliably detected, which is important since these patients can be considered for thrombectomy. While sensitivity is in the range previously reported for neuroradiologists, the specificity is much lower than that of experienced human readers. The algorithm should therefore be used as a screening tool to expedite diagnosis rather than a surrogate for an experienced human reader. Fast processing times make its use feasible in the emergent clinical setting.

## Sources of Funding

None.

## Disclosures

Professor Bammer is a shareholder of iSchemaView, which produces the RAPID CTA software, and HobbitView, Inc, an entity unrelated to this work. Dr Straka is also an iSchemaView shareholder and receives salary support. He has a patent AIF Selection Algorithm, issued and licensed by iSchemaView, Inc, CA. Professor Bammer and Dr Straka have a patent pending for Automated LVO detection on CTA. Their role in this study was strictly limited to software development and support and statistical tests. Dr Dehkharghani is a

consultant to iSchemaview. Dr Amukotuwa has a relationship with one of the founders of iSchemaView but receives no financial support and has no equity. Professor Fischbein, Dr Chandra, and H. Smith have no conflicts of interest to declare.

## References

1. Malhotra K, Gornbein J, Saver JL. Ischemic strokes due to large-vessel occlusions contribute disproportionately to stroke-related dependence and death: a review. *Front Neurol*. 2017;8:651. doi: 10.3389/fneur.2017.00651
2. Goyal M, Menon BK, van Zwam WH, Dippel DW, Mitchell PJ, Demchuk AM, et al; HERMES collaborators. Endovascular thrombectomy after large-vessel ischaemic stroke: a meta-analysis of individual patient data from five randomised trials. *Lancet*. 2016;387:1723–1731. doi: 10.1016/S0140-6736(16)00163-X
3. Lin Y, Schulze V, Brockmeyer M, Parco C, Karathanos A, Heinen Y, et al. Endovascular thrombectomy as a means to improve survival in acute ischemic stroke: a meta-analysis. *JAMA Neurol*. 2019;76:850–854. doi: 10.1001/jamaneurol.2019.0525
4. Albers GW, Marks MP, Kemp S, Christensen S, Tsai JP, Ortega-Gutierrez S, et al; DEFUSE 3 Investigators. Thrombectomy for stroke at 6 to 16 hours with selection by perfusion imaging. *N Engl J Med*. 2018;378:708–718. doi: 10.1056/NEJMoa1713973
5. Nogueira RG, Jadhav AP, Haussen DC, Bonafe A, Budzik RF, Bhuva P, et al; DAWN Trial Investigators. Thrombectomy 6 to 24 hours after stroke with a mismatch between deficit and infarct. *N Engl J Med*. 2018;378:11–21. doi: 10.1056/NEJMoa1706442
6. Powers WJ, Rabinstein AA, Ackerson T, Adeoye OM, Bambakidis NC, Becker K, et al; American Heart Association Stroke Council. 2018 Guidelines for the early management of patients with acute ischemic stroke: a guideline for healthcare professionals from the American Heart Association/American Stroke Association. *Stroke*. 2018;49:e46–e110. doi: 10.1161/STR.0000000000000158
7. Campbell BC, Mitchell PJ, Kleinig TJ, Dewey HM, Churilov L, Yassi N, et al; EXTEND-IA Investigators. Endovascular therapy for ischemic stroke with perfusion-imaging selection. *N Engl J Med*. 2015;372:1009–1018. doi: 10.1056/NEJMoa1414792
8. Goyal M, Demchuk AM, Menon BK, Eesa M, Rempel JL, Thornton J, et al; ESCAPE Trial Investigators. Randomized assessment of rapid endovascular treatment of ischemic stroke. *N Engl J Med*. 2015;372:1019–1030. doi: 10.1056/NEJMoa1414905
9. Saver JL, Goyal M, Bonafe A, Diener HC, Levy EI, Pereira VM, et al; SWIFT PRIME Investigators. Stent-retriever thrombectomy after intravenous t-PA vs. t-PA alone in stroke. *N Engl J Med*. 2015;372:2285–2295. doi: 10.1056/NEJMoa1415061
10. Campbell BC, Yassi N, Ma H, Sharma G, Salinas S, Churilov L, et al. Imaging selection in ischemic stroke: feasibility of automated CT-perfusion analysis. *Int J Stroke*. 2015;10:51–54. doi: 10.1111/ijis.12381
11. Lansberg MG, Straka M, Kemp S, Mlynash M, Wechsler LR, Jovin TG, et al; DEFUSE 2 Study Investigators. MRI profile and response to endovascular reperfusion after stroke (DEFUSE 2): a prospective cohort study. *Lancet Neurol*. 2012;11:860–867. doi: 10.1016/S1474-4422(12)70203-X
12. Lansberg MG, Lee J, Christensen S, Straka M, De Silva DA, Mlynash M, et al. RAPID automated patient selection for reperfusion therapy: a pooled analysis of the Echoplanar Imaging Thrombolytic Evaluation Trial (EPITHET) and the Diffusion and Perfusion Imaging Evaluation for Understanding Stroke Evolution (DEFUSE) Study. *Stroke*. 2011;42:1608–1614. doi: 10.1161/STROKEAHA.110.609008
13. Bouthillier A, van Loveren HR, Keller JT. Segments of the internal carotid artery: a new classification. *Neurosurgery*. 1996;38:425–432; discussion 432. doi: 10.1097/00006123-199603000-00001
14. Goyal M, Menon BK, Krings T, Patil S, Qazi E, McTaggart RA, et al. What constitutes the M1 segment of the middle cerebral artery? *J Neurointerv Surg*. 2016;8:1273–1277. doi: 10.1136/neurintsurg-2015-012191
15. Becks MJ, Manniesing R, Vister J, Pegge SAH, Steens SCA, van Dijk EJ, et al. Brain CT perfusion improves intracranial vessel occlusion detection on CT angiography. *J Neuroradiol*. 2019;46:124–129. doi: 10.1016/j.neurad.2018.03.003
16. Lev MH, Farkas J, Rodriguez VR, Schwamm LH, Hunter GJ, Putman CM, et al. CT angiography in the rapid triage of patients with hyperacute stroke to intraarterial thrombolysis: accuracy in the detection of large vessel thrombus. *J Comput Assist Tomogr*. 2001;25:520–528.



17. Wagemans BA, van Zwam WH, Nelemans PJ, van Oostenbrugge RJ, Postma AA. 4D-CTA improves diagnostic certainty and accuracy in the detection of proximal intracranial anterior circulation occlusion in acute ischemic stroke. *PLoS One*. 2017;12:e0172356. doi: 10.1371/journal.pone.0172356
18. Barreira CM, Bouslama M, Lim J, Al-Bayati AR, Haussen D, Grossberg J, et al. As10-047: Aladin study: automated large artery occlusion detection in stroke imaging study - a multi-center experience. *European Stroke Journal*. 2018;3 (IS).
19. Barreira CM, Bouslama M, Haussen DC. Abstract wp61: automated large artery occlusion detection in stroke imaging - aladin study. *Stroke*. 2018;49(suppl 1).
20. Rocha M, Jovin TG. Fast versus slow progressors of infarct growth in large vessel occlusion stroke: Clinical and research implications. *Stroke*. 2017;48:2621–2627. doi: 10.1161/STROKEAHA.117.017673
21. Campbell BC, Christensen S, Tress BM, Churilov L, Desmond PM, Parsons MW, et al; EPITHET Investigators. Failure of collateral blood flow is associated with infarct growth in ischemic stroke. *J Cereb Blood Flow Metab*. 2013;33:1168–1172. doi: 10.1038/jcbfm.2013.77
22. Sarraj A, Sangha N, Hussain MS, Wisco D, Vora N, Eljovich L, et al. Endovascular therapy for acute ischemic stroke with occlusion of the middle cerebral artery M2 segment. *JAMA Neurol*. 2016;73:1291–1296. doi: 10.1001/jamaneurol.2016.2773